ACS OMEGA

http://pubs.acs.org/journal/acsodf

Article

Response Surface Methodology for the Synthesis and Characterization of Bio-Oil Extracted from Biomass Waste and Upgradation Using the Rice Husk Ash Catalyst

Muhammad Irfan, Syed Ali Ghalib,* Sharjeel Waqas, Javed Akbar Khan, Saifur Rahman, Salim Nasar Faraj Mursal, and Abdulnour Ali Jazem Ghanim

Cite This: *ACS Omega* 2023, 8, 17869−17879

Read Online

ACCESS | Metrics & More | Article Recommendations

ABSTRACT: Rice husk ash (RHA), a low-cost biomaterial, was utilized to form bio-oil from pyrolysis in a batch-stirred reactor, followed by its upgradation using the RHA catalyst. In the present study, the effect of temperature (ranging from 400 to 480 °C) on bio-oil production produced from RHA was studied to obtain the maximum bio-oil yield. Response surface methodology (RSM) was applied to investigate the effect of operational parameters (temperature, heating rate, and particle size) on the bio-oil yield. The results showed that a maximum bio-oil output of 20.33% was obtained at 480 °C temperature, 80 °C/min heating rate, and 200 μm particle size. Temperature and heating rate positively impact the bio-oil yield, while particle size has little effect. The overall R^2 value of 0.9614 for the proposed model proved in good agreement with the experimental data. The physical properties of raw bio-oil were determined, and 1030 kg/m^3 density, 12 MJ/kg calorific value, 1.40 cSt viscosity, 3 pH, and 72 mg KOH/g acid value were obtained, respectively. To enhance the characteristics of the bio-oil, upgradation was performed using the RHA catalyst through the esterification process. The upgraded bio-oil stemmed from a density of 0.98 g/cm^3, an acid value of 58 mg of KOH/g, a calorific value of 16 MJ/kg, and a viscosity 10.5 cSt, respectively. The physical properties, GC−MS and FTIR, showed an improvement in the bio-oil characterization. The findings of this study indicate that RHA can be used as an alternative source for bio-oil production to create a more sustainable and cleaner environment.

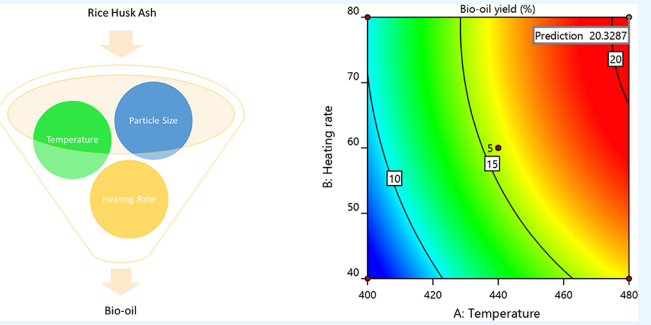

1. INTRODUCTION

Biomass waste is a promising source of renewable energy that can be used to replace fossil fuels that are running out. It is cost-effective, easily biodegradable, carbon-neutral, and emits little greenhouse gas.[1,2] The energy generation from biomass includes thermochemical techniques to produce bio-oil through pyrolysis. Biomass waste is converted into bio-oil or syngas by the thermochemical process of pyrolysis.[2,3] Pyrolysis has been developed considerably as an alternative technique for efficiently converting low-cost biomass into a liquid product that can be potentially used to replace conventional fossil fuels.[4] Pyrolysis is environmentally feasible and has the benefit of low operational costs. The high bio-oil productivity from the low-cost biomass has opened the doors to numerous industrial applications.[5,6]

Rice husk ash (RHA) is a solid residue formed when rice husk decomposes. RHA is suitable for pyrolysis because it has a high mesoporous surface area and silica content.[7] The RHA catalytic process can enhance bio-oil physical properties (acid value, caloric value, density, and viscosity).[8] RHA pyrolysis produces high bio-oil quantity at elevated temperatures (450−500 °C). Bakar and Titiloye[5] recommended that RHA could enhance gaseous product yield to 21.6 wt % at a modest temperature of 500 °C. Abbas et al.[9] studied pyrolysis of RHA and found optimal biochar and bio-oil yields of 39 and 19%, respectively, at 500 °C. Acid values and carboxyl groups drastically reduced at higher temperatures (700 °C), while biochar produced at higher temperatures was highly stable. At temperatures ranging from 400 to 500 °C and a heating rate of 60 °C/min, Natarajan[10] explored RHA pyrolysis at a slow rate. The resultant product contains 22.5 to 31.7% of liquid compounds, 27.7 to 42.5% of gaseous compounds, and 34.1 to 42.5% of solids. Cao et al.[11] studied the synthesis of biochar to develop an effective catalyst for chemical synthesis. Gui et al.[12] evaluated the fast and slow pyrolyzed bio-oil production process, focusing on temperature,

Received: February 10, 2023
Accepted: April 28, 2023
Published: May 11, 2023

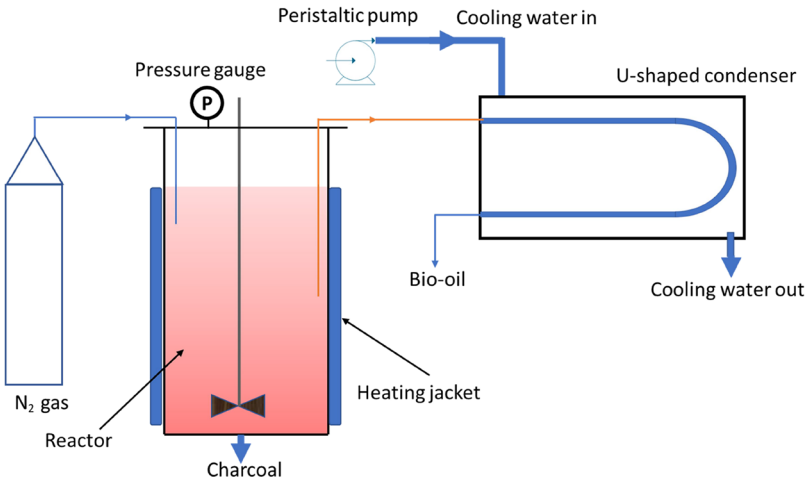

Figure 1. Schematic diagram of the batch stirred reactor.

heating rate, and yield. The study evaluates the coconut shells, RHA, and 50% of each constituent to create the benchmarks. Islam et al.[13] evaluated the highest yield parameters for bio-oil synthesis utilizing solid waste in a 500 °C fixed bed reactor. The product analysis shows 30% of liquid products and 33% of solid products are produced from the pyrolysis of RHA. Furthermore, low investment cost, ease of operation, and secondary reaction probation make it an attractive choice.[14] However, there is limited literature related to the RHA performance for the enhancement of properties.[8]

The bioreactor's performance can be more efficient with the help of optimization and the correlation of the operational parameters.[15] Therefore, to optimize the parameters, the design of experiments (DOE) can be useful for being statistically foreseeable because of its ability to give highly reliable results with fewer experiments.[16,17] Response surface methodology (RSM) is an exceptional approach to increasing the efficiency of the reactors' performance and studying different parameters' behaviors simultaneously.[18] RSM is an experiential statistical technique that can help understand the mutual relationship of several process parameters by investigating the mathematical modeling on the response variable.[19] The quantitative data acquired from experimental design, regression model analysis, and operational conditions can result in high-end performance.[20] A number of studies concentrate on improving the operating conditions of the bio-oil yield. Several parameter operating systems can be optimized by applying the RSM design at the cost of maximum bio-oil production.[15,18]

To replicate conventional fossil fuels, bio-oil needs to address the issues of small calorific value and elevated acid value. Poor consistency and stability also limit the high-grade application of bio-oil.[21] The high quantity of organic acids is the major cause of the elevated acid value, reduced stability, and corrosiveness of bio-oil.[8] Therefore, the upgradation of bio-oil is required before industrial applications to obtain a higher-efficiency fuel. The upgradation of bio-oil enhances the physical properties, increasing performance efficiency and stability. The current upgradation practices include catalytic esterification, catalytic hydrogenation, and catalytic cracking. The main goal of these upgradation techniques is to decrease the quantity of organic acids (acetic acid, formic acid, and propionic acid) to increase the stability and physical properties.

The catalytic esterification reaction is an upgradation process of bio-oil that converts carboxylic acids to esters. It reduces the acid value and corrosiveness of the bio-oil bit. It prohibits some secondary reactions catalyzed by these acids, e.g., the homopolymerization reaction of aldehyde phenol/aldehyde polymerization reactions. Limited studies have been reported on the catalytic esterification of bio-oil; this technique is still a subject of attention.[22] Therefore, this study aims to enhance bio-oil properties using catalytic esterification to upgrade the bio-oil.

The current research aims to study bio-oil production through pyrolysis from an indigenous sample of RHA, and the effect of temperature is studied for bio-oil maximum output. RSM has been applied to investigate operational parameters' impact on the bio-oil yield and optimization. The upgradation of the produced bio-oil was performed through the esterification reaction to enhance the physical properties.

2. MATERIALS AND METHODS

2.1. Raw Materials. The source of RHA was Bismillah Sheller Jaranwala, Punjab, Pakistan. Other chemicals used in the experiments are potassium hydroxide (100%), sulfuric acid (98 wt %), and methanol (analytical grade), which were acquired from Merck. All the chemicals were used as received without any further treatment. According to the ASTM standards, the proximate analysis of RHA was carried out.

2.2. Pre-Treatment of RHA. The first step in preparing RHA samples for pyrolysis is obtaining a uniform particle size. RHA was grounded and sieved so that 80% of the sample passed through a 200 μm sieve. The grinding and sieving of the raw samples were done to cater to the size requirement of the pyrolysis equipment.

2.3. Pyrolysis Equipment and Start-Up. The pyrolysis equipment comprises an external heater and a stainless-steel reactor enabled by a mechanical stirrer, as shown in Figure 1. Thermocouples were installed on the reactor to determine the reactor temperature. The pyrolysis reactor was insulated to minimize heat losses. Pyrolysis was conducted without oxygen, so nitrogen gas guaranteed an inert atmosphere. A steady flow of nitrogen was provided at the beginning of each experiment. At the start, nitrogen gas was set at a 100 mL/min flow rate, reducing as the experiment progresses. The final setpoint for nitrogen gas is 10 mL/min. The continuous supply of nitrogen gas helps to maintain the inert environment. The inert environment facilitates the pyrolysis process by preventing secondary reactions. The temperature setpoint was set through a temperature controller, and the reactor attained the steady-state

https://doi.org/10.1021/acsomega.3c00868
ACS Omega 2023, 8, 17869−17879

condition. The known amount of RHA sample was put in the reactor, the lid was sealed, and the pyrolysis process started. The experiments were carried out in triplicates to ensure accuracy for five different temperatures that ranged from 400 to 480 °C. After the pyrolysis, the liquid product is obtained while char is gathered from the bottom. Through the flue, all the gaseous products were vented out. The top products flowed through a condenser facilitated with cold water. The gaseous products flowed through the condenser on the shell side while cooling water was provided inside the tubes. The vapors were condensed to form bio-oil. The solid products of the pyrolysis gathered at the bottom of the reactor. The solid products known as biochar were collected from the reactor.

2.4. Catalyst Preparation. RHA was grounded and sieved so that 80% of the sample passed through a 200 μm sieve. The prepared sample was washed with 0.1 mol/L hydrochloric acid solutions for 1 h. The grounded sample can contain some impurities, and hydrochloric acid is very useful for their removal. The hydrochloric acid solution removes the traces of metals, organic compounds, and minerals contained in RHA. The prepared sample was neutralized. To get rid of all the traces of hydrochloric acid, the sample was rinsed thoroughly with water. The sample was allowed to dry at ambient temperature before being dehydrated for 2 h at 105 °C. 6 g of RHA was added in 100 mL of concentrated sulfuric acid (98%) into a Teflon tube autoclave for sulfonation. The Teflon tube autoclave was then put into an oven at 145 °C for 12 h. The sample was washed with deionized water and filtrated through 0.45 μm filter paper to eliminate excess sulfate ions. The solution was then dried in the oven to remove the moisture content.

2.5. Esterification Reaction. Bio-oil produced from RHA from the pyrolysis process was used in the esterification reaction. RHA (4 wt % of raw bio-oil) and 20 wt % of methanol were used for the esterification reaction at 60 °C temperature for 90 min. After the completion of the reaction time, the final product was centrifuged for 2 h and the sample was separated into organic and aqueous phases. The separated phases (organic and aqueous) were collected and evaluated separately. The raw and upgraded bio-oil were characterized through FTIR and GC−MS to determine the relative composition. The physical properties such as acid value, density, kinematic viscosity, and calorific values were determined.

2.6. Proximate Analysis of RHA. The following physical properties were measured for the proximate analysis of RHA.

2.6.1. Moisture Content. The moisture content in RHA was calculated according to ASTM D-3173; 1 g of RHA was dried in the oven for 1 h at 100 °C. The sample was weighed before and after to determine the weight loss due to the vaporization of moisture content. The moisture content was determined using eq 1.

$$M_c = \frac{W_i - W_f}{W_i} \times 100 \quad (1)$$

where M_c is the moisture content in the RHA sample (%), W_i is the initial weight (g), and W_f is the final weight (g).

2.6.2. Ash Content. 1 g of sample was placed in the muffle furnace at 750 °C for 90 min. The initial sample and final ash weights were measured, and ash content was calculated using eq 2.

$$A_c = \frac{A_o}{W_i} \times 100 \quad (2)$$

where A_c is the ash content (%), A_o the mass of ash (g), and W_i is the initial mass of the sample (g).

2.6.3. Volatile Matter. A crucible furnace was used to calculate the volatile matters according to ASTM D 3175. One gram of RHA was put in the furnace for 7 min at 925 °C. The sample was removed, and the final weight of the sample was done again. Volatile matter can be calculated using eq 3.

$$V_M = \frac{W_L}{W_i} \times 100 \quad (3)$$

where V_M is the volatile matter content (%), W_L is the loss of mass due to volatile matter (g), and W_i is the initial mass of the sample (g).

2.6.4. Fixed Carbon. By adding all the values calculated above and then subtracting them from 100, the fixed carbon was determined once the volatile matter, ash, and moisture contents were obtained, as described in eq 4.

$$F_C = 100 - (M_C + A_C + V_M) \quad (4)$$

2.7. Product Characterization. The various techniques were used to characterize both the raw and upgraded bio-oil techniques. Both viscosity and density were calculated through standard methods.[23] The calorific value was calculated utilizing an IKA C 5000 bomb calorimeter.

2.8. Experimental Design Using the Response Surface Methodology Method. Using statistical and mathematical approaches, RSM scrutinizes the effect of various operational parameters on the response function. RSM optimizes the response function and deducts the heightened operational parameter values. To study the effect of different *operational* parameters on the bio-oil yield, a *three*-level Box−Behnken design (BBD) was implemented with three numeric factors. *Seventeen* runs were performed for the three operational parameters temperature, heating rate, and particle size, with five center points per block. The *three*-level BBD consists of a low level (−1), *a* medium level (0), and *a* high level (−1). The temperature varied from 400 *to* 480 °C, the heating rate inside the reactor was changed from 40−80 °C/min, *and* the particle size of the feed RHA was changed from 100 *to* 200 μm, as shown in Table 1.

Table 1. Three-Level Box−Behnken Design for the Three Operational Parameters

levels	independent variable	unit	low level (−1)	medium level (0)	high level (+1)
1	temperature	°C	400	440	480
2	heating rate	°C/min	40	60	80
3	particle size	μm	100	200	300

3. RESULTS AND DISCUSSION

3.1. Characterization of Raw Material. The proximate and ultimate analysis of RHA depicts the properties described in Table 2. The raw RHA contains 11.67% moisture, 14.56% ash, and 56.32% volatile matter. The calorific value of the raw RHA is 2.06 MJ/kg, and the fixed carbon content is 17.45%. The raw RHA's high value of fixed carbon content exhibits a high biochar yield. Contrarily, volatile matter and ash content adversely affect the biochar yield. The ultimate analysis of RHA revealed a carbon content of 38.4 ± 0.2%, hydrogen 5.5 ± 0.1%, nitrogen 1.2 ± 0.1%, and oxygen 54.9 ± 0.2%, respectively.

https://doi.org/10.1021/acsomega.3c00868
ACS Omega 2023, 8, 17869−17879

Table 2. Properties of the Raw Material

type	property	value
proximate analysis	moisture contents (%)	11.67
	volatile matters (%)	56.32
	ash contents (%)	14.56
	fixed carbon (%)	17.45
	calorific value	2.06 MJ/kg
ultimate analysis	carbon (%)	38.4 ± 0.2
	hydrogen (%)	5.5 ± 0.1
	nitrogen (%)	1.2 ± 0.1
	oxygen (%)	54.9 ± 0.2

A high ash content results in a low calorific value of the producer gas.[24] Ash content is the inorganic content that is left behind after combustion. A low carbon content value and a high volatile matter result in higher quantities of producer gas.[25] The fixed carbon is the amount of carbon available for combustion during pyrolysis. A fixed carbon value of 17.45% indicates a low resistance to the degradation process and low heat release during combustion. The moisture content of 11.67% is within the recommended limit of 15%, as described in ref 26. A high value of ash and moisture contents renders a calorific value. The volatile matter is released when heated to a high temperature (<400 °C). The volatile matter decomposes to produce volatile gases and solid biochar. RHA typically has a high volatile content (up to 80%). A volatile matter of 56.32% was recorded for RHA that depicts easy ignition and higher flame efficiency. A low volatile matter is also beneficial for a high product yield. The low calorific value of RHA was due to high moisture content and volatile matter. However, the calorific value is sufficient to produce heat for small-scale applications.

3.2. Influence of Temperature on Bio-Oil and Biochar Yield. The temperature range defines the type of pyrolysis applied in the specific system. Slow pyrolysis occurs at temperatures between 250 and 400 °C, whereas intermediate pyrolysis occurs at temperatures between 400 and 500 °C. A higher temperature range implies a fast pyrolysis process. All these processes are differentiated by different chemical reactions at different temperatures. The pyrolysis of RHA was conducted at various temperatures (400−480 °C). The temperature range was selected based on the literature on similar raw materials, ensuring that the highest disintegration happens at the temperature limit of 400−500 °C.[27] However, due to system limitations, 480 °C is the maximum temperature limit for the current study.

The synthesis of bio-oil and biochar at various temperatures is depicted in Table 3. For RHA, the highest bio-oil production was acquired at 460 °C (19.45%), while the maximum biochar was accomplished at 400 °C (54.39%). With the temperature rise, bio-oil yield increases while biochar production decreases. Biomass is converted into biochar at low temperatures, thanks to the charring reactions. An upsurge in temperature results in the occurrence of de-volatilization reactions. These reactions release more volatile compounds, increasing production.[27] Beyond 460 °C, the volatile matter undergoes secondary cracking reactions, thus increasing non-condensable gases and decreasing bio-oil production. Various researchers have described identical findings using similar raw materials.[28]

Table 3. Pyrolysis of RHA at Different Temperatures

sr. no.	temperature (°C)	bio-oil yield (%)	biochar yield (%)
1	400	8.38	54.39
2	420	10.97	49.33
3	440	15.79	45.78
4	460	19.45	43.46
5	480	17.34	46.49

3.3. Model Development and Statistical Analysis Using Response Surface Methodology. *Seventeen* experiments were designed using the DOE.[17] The results of experiments in bio-oil yield are shown in Table 4. A *three*-level BBD model predicted the bio-oil yield against each experimental run.

Table 4. Pyrolysis of RHA at Different Operating Parameters for the Bio-Oil Yield

	operational parameters			bio-oil yield (%)	
run	temperature (°C)	heating rate (°C/min)	particle size (μm)	experimental value	predicted value
1	480	80	200	19.23	20.33
2	400	60	300	8	7.94
3	440	60	200	15	15.64
4	440	80	300	16.5	15.40
5	400	40	200	7	5.90
6	440	40	300	10	11.16
7	440	60	200	15.8	15.64
8	440	40	100	10.5	11.60
9	440	60	200	15.79	15.64
10	440	80	100	16.75	15.59
11	480	60	100	18.5	18.56
12	480	40	200	17.5	16.34
13	440	60	200	15.8	15.64
14	400	60	100	8.2	8.20
15	480	60	300	18.2	18.20
16	400	80	200	9	10.16
17	440	60	200	15.8	15.64

The coded and actual factors for the bio-oil yield are given in eqs 5 and (6).

$$\begin{aligned}\text{bio}-\text{oil yield (\%)} &= 15.64 + 5.15 \times A + 2.06 \times B - 0.1562 \times C \\ &\quad - 0.0675 \times \text{AB} - 0.0250 \times AC + 0.0625\, BC \\ &\quad - 1.33 \times A^2 - 1.12 \times \text{B}^2 - 1.08 \times C^2 \end{aligned} \tag{5}$$

$$\begin{aligned}\text{bio}-\text{oil yield (\%)} &= -225.14675 + 0.868856 \times \text{temperature} \\ &\quad + 0.470325 \times \text{heating rate} + 0.042472 \\ &\quad \times \text{particle size} - 0.000084 \times \text{temperature} \\ &\quad \times \text{heating rate} - 6.25 \times 10^{-6} \times \text{temperature} \\ &\quad \times \text{particle size} + 0.000031 \times \text{heating rate} \\ &\quad \times \text{particle size} - 0.000834 \times \text{temperature}^2 \\ &\quad - 0.002804 \times \text{heating rate}^2 - 0.000108 \\ &\quad \times \text{particle size}^2 \end{aligned} \tag{6}$$

The quadratic model has the highest R^2 value of 0.9614, as shown in Table 5. An R^2 value near 1 implicates that the model is significant. The *p*-values of the model parameters should be less than 0.05. A *p*-value <0.05 shows that the model term is

https://doi.org/10.1021/acsomega.3c00868
ACS Omega 2023, 8, 17869−17879

Table 5. Results of the Modeled Parameters

source	sum of squares	df	mean square	*F*-value	*p*-value	
model	266.42	9	29.60	19.38	0.0004	significant
A—temperature	212.49	1	212.49	139.10	<0.0001	
B—heating rate	33.95	1	33.95	22.22	0.0022	
C—particle size	0.1953	1	0.1953	0.1279	0.7312	
AB	0.0182	1	0.0182	0.0119	0.9161	
AC	0.0025	1	0.0025	0.0016	0.9689	
BC	0.0156	1	0.0156	0.0102	0.9223	
A^2	7.49	1	7.49	4.90	0.0624	
B^2	5.30	1	5.30	3.47	0.1049	
C^2	4.90	1	4.90	3.21	0.1163	
residual	10.69	7	1.53			
lack of fit	10.18	3	3.39	26.68	0.0042	significant
pure error	0.5089	4	0.1272			
cor total	277.11	16				
other statistical parameters						
R^2	adjusted R^2	S.D.	A.P.	C.V. (%)		
0.9614	0.9118	1.24	15.22	8.84		

significant. In the current quadratic model, the temperature and heating rate are significant parameters with *p*-values <0.05, while particle size is insignificant. Figure 2 shows the comparison of the actual vs predicted plot. The close relationship between the predicted and actual values shows the model's effectiveness.

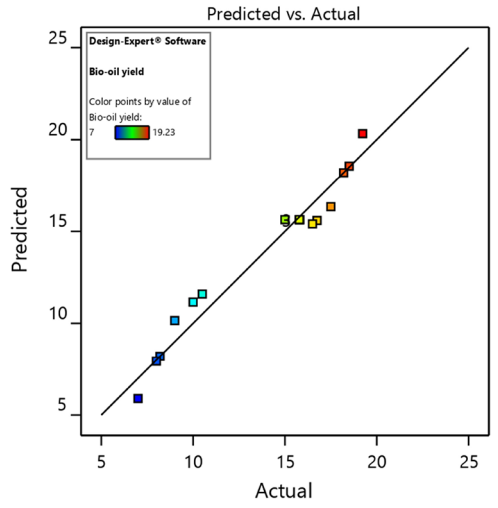

Figure 2. Actual vs predicted plot for the bio-oil yield.

3.4. Process Analysis. Figure 3 shows the impact of operational parameters (temperature, heating rate, and particle size) on the bio-oil yield. Figure 3a,b shows that the temperature and heating rate positively impact bio-oil production. A higher value of temperature and heating rate facilitates higher bio-oil yield. Isa et al.[29] investigated the temperature impact and observed that maximum production is achieved at 473.37 °C. Park et al.[30] explored the bio-oil yield for the sewage sludge and found *that* the highest bio-oil production was accomplished at 450 °C. Heo et al.[31] researched the sawdust for the optimum operating conditions and found the highest bio-oil produced at 450 °C.

Figure 3c,d demonstrates the effect of temperature and particle size. The particle size of the input feed is an important parameter. The smaller particle size increases the heat transfer rate resulting in higher product efficiency. A large particle size hinders uniform heat distribution and slows pyrolysis. The results show that a particle size of 100 μm yields the maximum bio-oil production. However, the impact of particle size is insignificant because of the fixed bed system. The same effect is shown in Figure 3e,f.

3.5. Process Optimization. The maximum bio-oil yield was selected for the optimal operational parameter selection. Figure 4 shows a maximum bio-oil yield of 20.33% obtained at 480 °C temperature, 80 °C/min heating rate, and 100 μm particle size, respectively. The model's degree of desirability is one under these operating conditions.

3.6. Bio-Oil Properties. The physical parameters of the bio-oil obtained from the pyrolysis of RHA are listed in Table 6. It depicts raw bio-oil properties containing density, calorific value, acid number, pH, and kinematic viscosity. Physical properties are a significant tool to describe the produced bio-oil quality. The acid number for the raw bio-oil was noticeably high, with 72 mg KOH/g. The high acid number value is common for raw bio-oil. The catalytic conversion of RHA or upgradation of bio-oil can reduce the acid number to 39−47 mg KOH/g.[5] Acetic acid is a major contributor to the acid number; however, carboxylic acid, phenols, and other acidic compounds contribute significantly.[5] The pH is acidic, and the value is 3. The acidic pH and high acid number value indicate a vague relationship. Bio-oil has an oil and aqueous phase, and pH is a measure of hydrogen ions in an aqueous solution.[32] However, the literature indicates no correlation between pH and acid number.[33] The acid number measurement is related to the acidity measurement than the pH, considering the aqueous and organic phases.

The physical parameters of the bio-oil generated are listed in Table 2. It describes the density and water content of 1030 kg/m^3 and 52.3%, respectively. The water content indicates dehydration and cracking reactions. The water content percentage shows the dehydration tendency associated with the acid number.[34] Ji-Lu[35] observed the density and water content of 1190 kg/m^3 and 25.2%, respectively, for the RHA-produced bio-oil. Lu et al.[36] achieved a density of 1140 kg/m^3 and 28% water content. The kinematic viscosity of the bio-oil shows its highest value at 1.40 cSt.

3.7. Bio-Oil Upgradation. Upgradation was performed through esterification to enhance the characteristics, as shown in Table 7. The water percentage and low calorific value render its

https://doi.org/10.1021/acsomega.3c00868
ACS Omega 2023, 8, 17869−17879

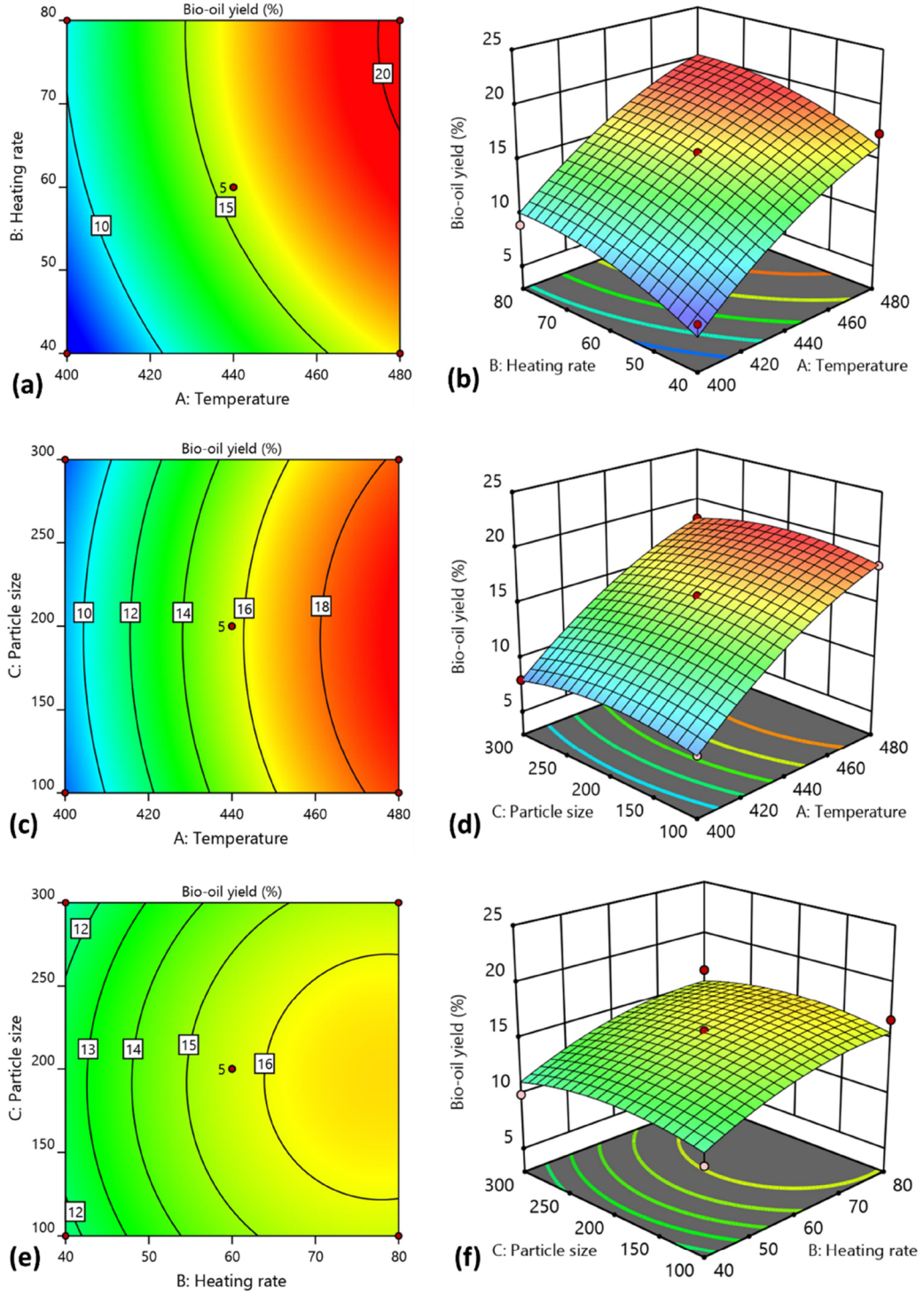

Figure 3. The effect of operational parameters on the bio-oil yield in the form of the 2D counter of (a) temperature and heating rate, (b) temperature and particle rate, and (c) heating rate and particle size and 3D response surface plots of (d) temperature and heating rate, (e) temperature and particle rate, and (f) heating rate and particle size.

use for commercial purposes.[37] The physical properties are described in Table 6. Bio-oil has a pH range of 3.5 to 5, suggesting that it is very damaging. Sharpness and the destructive nature result from a high concentration of greasy acids. Furthermore, the side reactions might persist during the capacity period; for example, polymerization and dissipation of these side reactions will produce a modest increase in width.

The low net heat value of the bio-oil limits its widespread applications as an alternative to conventional fossil fuels. The heat value of biomass pyrolysis ranges from 15 to 19 MJ/kg. The pyrolysis produced bio-oil with a heat value of 12.51 MJ/kg. The low heating value is associated with crude oil (42 MJ/kg). On the other hand, bio-oils must fulfill specified viscosity benchmarks. At 40 °C, the consistency of gas turbine oil is typically between 2.5 and 30 mm^2/s. The upgraded oil has a viscosity of

https://doi.org/10.1021/acsomega.3c00868
ACS Omega 2023, 8, 17869−17879

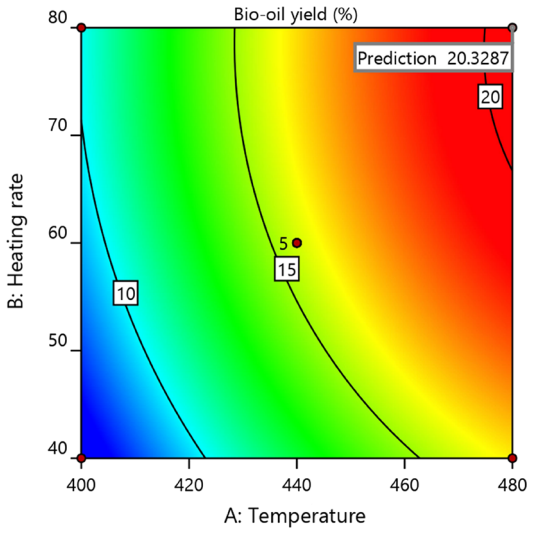

Figure 4. Value of optimized operational parameters at maximum bio-oil yield.

Table 6. Physical Properties of Raw Bio-Oil.

sr. no.	physical property	unit	value
1	density	kg/m^3	1030
2	calorific value	MJ/kg	12
3	acid value	mg KOH/g	72
4	pH		3
5	kinematic viscosity	cSt	1.40
6	water content	%	52.3

Table 7. Physical Characteristics of Upgraded Bio-Oil.

sr. no.	physical characteristic	unit	upgraded bio-oil
1	density	kg/m^3	980
2	calorific value	MJ/kg	16
3	acid value	mg KOH/g	54
4	pH		4.8
5	kinematic viscosity	cSt	1.05
6	water content	%	47.4

1.05 cSt at 40 °C, partitioned by thickness, far too high for gas turbines. Mixing bio-oil with natural dissolvable (methanol, ethanol) can decrease consistency.[38]

This study employed esterification for the upgradation of bio-oil produced from biomass pyrolysis. After esterification, the acid value decreased from 72 to 54 mg KOH/g for the upgraded bio-oil. The decrease in acid value can be ascribed to converting carbonyl compounds and alcohols to carboxylic acids. The esterification process results in carbonyl compounds and alcohol oxidation to stable compounds (carboxylic acids). The esterification increases the physical properties (acid, pH, calorific value), while density and kinematic viscosity remain the same.

Recent studies on RHA reveal the importance of bio-oil production through low-cost biodegradable compounds. Using a fluidized bed reactor to pyrolyze RHA improved bio-oil yield by using a lower pyrolysis temperature, higher feed rate, and longer residence time. It was also found that the bio-oil had a high heating value and low acidity, making it a potential alternative to fossil fuels.[39] The investigation on the effect of feedstock particle size on bio-oil yield and quality in RHA pyrolysis showed that smaller particle sizes resulted in higher bio-oil yields and a lower content of oxygenated compounds, which improved the quality of the bio-oil.[40] The use of an externally heated rotary kiln to pyrolyze RHA resulted in the optimal pyrolysis temperature of around 450 °C, and the bio-oil produced had a high heating value and low acidity.[41] The investigation on the use of microwave-assisted pyrolysis to produce bio-oil from RHA uncovered that the technique could significantly improve the bio-oil yield and reduce energy consumption compared to conventional pyrolysis.[42] The research on the effect of adding a small amount of calcium oxide (CaO) on the pyrolysis of RHA resulted that the addition of CaO significantly increased the bio-oil yield and improved the quality, reducing the acidity and increasing the heating value.[43] The exploration of catalytic pyrolysis to produce bio-oil from RHA using a zeolite catalyst discovered that the catalyst significantly increased the bio-oil yield and improved its quality, reducing the acidity and increasing the heating value.[44] Overall, these studies demonstrate ongoing research efforts to optimize the pyrolysis of RHA and explore new techniques to improve bio-oil yield and quality. The use of catalysts, microwave-assisted pyrolysis, and externally heated rotary kilns show promise for improving the efficiency and sustainability of bio-oil production from RHA.

3.8. FTIR Spectrum. Figure 5 illustrates the FTIR spectra, which show the presence of different bonding and functional groups. Characteristic vibrational modes observed at 1650 cm^{-1} show aromatic C=C bonding, while 3000−3400 cm^{-1} shows hydroxyl group (−OH) stretching and hydrogen bonding (H−H) present in 2500−3000 cm^{-1}.[45] The wavelength of 1000−1500 cm^{-1} demonstrates carbonyl groups, while 3000−3500 cm^{-1} indicates the occurrence of alkenes and alkynes. The various wavenumbers indicate the existence of C=C bonds, C=O bonds, C−H bonds, and O−H bonds in the raw bio-oil. These functional groups demonstrate the presence of aromatics, phenols, alcohols, and acids.

The absorbance top at around 1030 cm^{-1} was very noticeable, possibly due to the C−O occurrence. The C−O bowing and vibration at 1235 cm^{-1} originated in the algal waste spectra, which recommends the existence of fats and esters.[46] The FTIR spectra of upgraded bio-oil in the 1190−1750 cm^{-1} region could deliver comprehensive knowledge of various carbonyl groups' presence. The RHA biomass consists of cellulose, lignin, and hemicellulose, converting to carbonyl compounds upon pyrolysis.

3.9. GC−MS Analysis. GC−MS was used to investigate the level of bio-oil detachment or sub-atomic load. The working states of GC−MS are clarified in Table 8. The terminology of the samples was overseen as per the temperature of the catalyst. Each peak has a number that speaks to a particular compound having wealth at a particular residence time. These compounds have a place with a gathering of methyl esters and give us the affirmation of created bio-oil. Each look shows explicit plenitude with respect to its residence time, which implies that this compound is available in a specific sum. This sum was determined with the assistance of the region under the bend of that look removed from the information examination programming of GC−MS. The GC−MS result shows the presence of various classes of hydrocarbons, which incorporates azoles, aromatic amines and nitrites, sugar, alkenes, and alkane.

The compound organization of crude bio-oil and updated bio-oil was investigated by GC−MS (Table 8). Around 50 substance mixes were recognized by GC−MS, with some of the important ones mentioned here. As appeared in this segment, the

https://doi.org/10.1021/acsomega.3c00868
ACS Omega 2023, 8, 17869−17879

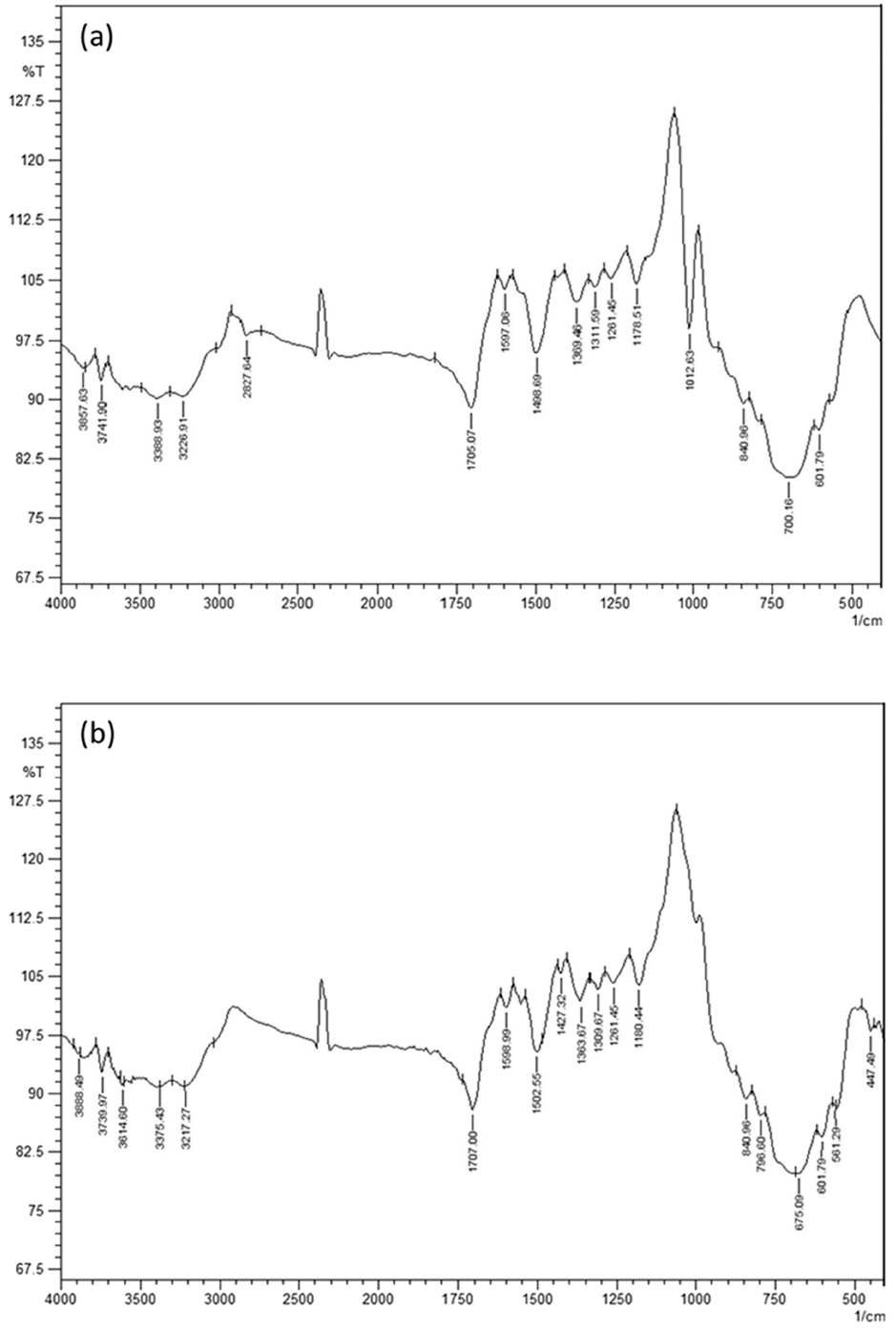

Figure 5. FTIR analysis of the (a) raw and (b) upgraded bio-oil.

significant substance intensifies present in the updated bio-oil are esters, ethers, ketones, phenols, and alcohols.

3.10. Comparison of Bio-Oil with Commercial Fuels.

Table 9 shows the comparison of bio-oil with commercial fuels, diesel, and gasoline. Bio-oil has a complex mixture of oxygenates, phenolics, ketones, and other compounds, while commercial fuel mainly consists of hydrocarbons. Bio-oil has a lower energy density, lower CN/ON, and higher viscosity compared to commercial fuel, but it has a higher flash point. The sulfur content of bio-oil varies, while commercial fuel has low sulfur content. Bio-oil has a lower environmental impact regarding CO_2 emissions, but it has the potential for high particulate matter emissions and other pollutants. Bio-oil is currently limited in availability compared to commercial fuel, which is widely available. The cost of bio-oil varies depending on the feedstock and production process used, while the cost of commercial fuel ranges from 0.5 to 1.8 USD/L. Overall, bio-oil is a promising renewable fuel source but currently has limitations in terms of energy density, availability, and cost compared to commercial fuel.

4. CONCLUSIONS

Pyrolysis of RHA to produce bio-oil is a promising technology for converting an agricultural waste product into a valuable energy source. The current research investigates the pyrolysis of RHA for bio-oil and its upgradation to ameliorate the properties.

https://doi.org/10.1021/acsomega.3c00868
ACS Omega 2023, 8, 17869−17879

Table 8. Physical Characteristics of Upgraded Bio-Oil.

raw bio-oil		upgraded bio-oil	
components	area	components	area
ethanone,1-(4- hydroxy-3-methoxyphenol)	19.35	1-butanol	34.25
phenol,2-methoxy-4-methyl-	10.91	acetic acid, butyl ester	8.79
acetic acid	5.20	propanoic acid, butyl ester	3.14
phenol,2-methoxy 2-propanone,1-hydroxy	4.11	butanoic acid, octyl ester	2.75
phenol,2-methoxy-3-(2-propenyl)-	3.21	phenol,4-methyl	2.71
phenol,2-methoxy-4-propyl-	3.18	cyclopentanone,2-methyl	2.39
phenol,4-ethyl-2-methoxy-	2.62	phenol,5-methoxy-2,3-dimethyl	2.15

The novelty of this research is upgradation through the esterification process to enhance its properties. Pyrolysis involves heating the RHA to high temperatures in the absence of oxygen, which produces a complex mixture of organic compounds, including bio-oil. The influence of temperature on pyrolysis showed that bio-oil production rises with an increase in temperature and vice versa for biochar. A maximum bio-oil yield of 19.45% was obtained at 460 °C, while a maximum bio-char yield of 54.39% was obtained at 400 °C. The biochar produced during pyrolysis is used for fuel briquettes. The RSM demonstrated that temperature and heating rate are the significant operational parameters affecting bio-oil yield. The maximum bio-oil yield of 20.33% was obtained at optimized operating parameter values of 480 °C temperature, 80 °C/min heating rate, and 200 μm particle size. The results demonstrated that the upgraded bio-oil significantly improves physical properties. The calorific value increased from 12 to 16 MJ/kg; the acid value decreased from 72 to 54 mg KOH/g and pH enhanced to 4.8, while kinematic viscosity changed to 1.05 cSt. The FTIR, GC−MS, and property measurement indicated that the upgradation experiment produced promising results. Overall, pyrolysis of RHA to produce bio-oil is a promising technology for converting agricultural waste into a valuable energy source. It has the potential to reduce dependence on fossil fuels and contribute to a more sustainable energy future.

AUTHOR INFORMATION

Corresponding Author

Syed Ali Ghalib − *Institute of Chemical Engineering and Technology, University of the Punjab, Lahore, Punjab 54590, Pakistan;* orcid.org/0009-0004-2273-5873; Email: alighalib.syad@gmail.com

Authors

Muhammad Irfan − *Electrical Engineering Department, College of Engineering, Najran University, Najran 61441, Saudi Arabia;* orcid.org/0000-0003-4161-6875

Sharjeel Waqas − *Chemical Engineering Department, Universiti Teknologi PETRONAS, Bandar Seri Iskandar 32610 Perak, Malaysia; School of Chemical Engineering, The University of Faisalabad, Faisalabad 37610, Pakistan*

Javed Akbar Khan − *Mechanical and Electrical Engineering Department, University of China Petroleum (East China), Dongying, Shandong 257061, China*

Saifur Rahman − *Electrical Engineering Department, College of Engineering, Najran University, Najran 61441, Saudi Arabia*

Salim Nasar Faraj Mursal − *Electrical Engineering Department, College of Engineering, Najran University, Najran 61441, Saudi Arabia*

Abdulnour Ali Jazem Ghanim − *Civil Engineering Department, College of Engineering, Najran University, Najran 61441, Saudi Arabia*

Complete contact information is available at: https://pubs.acs.org/10.1021/acsomega.3c00868

Author Contributions

S.A.G. and S.W. designed the study; data were collected by S.A.G.; and the literature was searched by S.W. and M.I. Original draft was written by S.A.G. and S.W. J.A.K., S.R., S.N.F.M., and A.A.J.G. helped in the preparation of some figures, revision of the manuscript. All authors approved the article for publication.

Notes

The authors declare no competing financial interest.

ACKNOWLEDGMENTS

Authors would like to acknowledge the support of the Deputy for Research and Innovation Ministry of Education, Kingdom of Saudi Arabia, for this research through grant (NU/IFC/02//

Table 9. A Comparative Table of the Bio-Oil with Diesel and Gasoline[47]

criteria	diesel fuel	gasoline	bio-oil
chemical composition	hydrocarbons (C8−C24) and additives	hydrocarbons (C4−C12) and additives	a complex mixture of oxygenates, phenolics, ketones, and other compounds
energy density (MJ/kg)	42.5	33.7	15−18
flash point (°C)	>62	−40	>75
cetane number (CN)	>40	not applicable	3−10
octane number (ON)	not applicable	>91	50−70
viscosity (cSt)	2−6	0.6−2.0	2−10
sulfur content (ppm)	<15	<10	varies
environmental impact	high emissions of NO_x and particulate matter	high emissions of volatile organic compounds (VOCs)	lower CO_2 emissions but the potential for high emissions of particulate matter and other pollutants
availability	widely available	widely available	limited availability
cost (USD/L)	0.5−1.5	0.7−1.8	varies, depending on the manufacturing process

https://doi.org/10.1021/acsomega.3c00868
ACS Omega 2023, 8, 17869−17879

SERC/-/017) under the Institutional Funding Committee at Najran University, Kingdom of Saudi Arabia.

REFERENCES

(1) Raheem, A.; Azlina, W. W.; Yap, Y. T.; Danquah, M. K.; Harun, R. Thermochemical conversion of microalgal biomass for biofuel production. *Renewable Sustainable Energy Rev.* **2015**, *49*, 990−999.
(2) Loy, A. C. M.; Gan, D. K. W.; Yusup, S.; Chin, B. L. F.; Lam, M. K.; Shahbaz, M.; Unrean, P.; Acda, M. N.; Rianawati, E. Thermogravimetric kinetic modelling of in-situ catalytic pyrolytic conversion of rice husk to bioenergy using rice hull ash catalyst. *Bioresour. Technol.* **2018**, *261*, 213−222.
(3) Amenaghawon, A. N.; Anyalewechi, C. L.; Okieimen, C. O.; Kusuma, H. S. Biomass pyrolysis technologies for value-added products: a state-of-the-art review. *Environment, Development and Sustainability* **2021**, *23*, 14324−14378.
(4) (a) Oasmaa, A.; Fonts, I.; Pelaez-Samaniego, M. R.; Garcia-Perez, M. E.; Garcia-Perez, M. Pyrolysis oil multiphase behavior and phase stability: a review. *Energy Fuels* **2016**, *30*, 6179−6200. (b) Fadhil, A. B. Production and characterization of liquid biofuels from locally available nonedible feedstocks. *Asia-Pac. J. Chem. Eng.* **2021**, *16*, No. e2572.
(5) Bakar, M. S. A.; Titiloye, J. O. Catalytic pyrolysis of rice husk for bio-oil production. *J. Anal. Appl. Pyrolysis* **2013**, *103*, 362−368.
(6) Aldobouni, I.; Fadhil, A.; Saied, I. Conversion of de-oiled castor seed cake into bio-oil and carbon adsorbents. *Energy Sources, Part A* **2015**, *37*, 2617−2624.
(7) (a) Prasara-A, J.; Gheewala, S. H. Sustainable utilization of rice husk ash from power plants: A review. *J. Cleaner Prod.* **2017**, *167*, 1020−1028. (b) Ong, H. C.; Chen, W.-H.; Farooq, A.; Gan, Y. Y.; Lee, K. T.; Ashokkumar, V. Catalytic thermochemical conversion of biomass for biofuel production: A comprehensive review. *Renewable Sustainable Energy Rev.* **2019**, *113*, No. 109266.
(8) Sutrisno, B.; Hidayat, A. Upgrading of bio-oil from the pyrolysis of biomass over the rice husk ash catalysts. In *IOP Conference Series: Materials Science and Engineering*, IOP Publishing 2016: Vol. *162*, p 012014.
(9) Abbas, Q.; Liu, G.; Yousaf, B.; Ali, M. U.; Ullah, H.; Munir, M. A. M.; Liu, R. Contrasting effects of operating conditions and biomass particle size on bulk characteristics and surface chemistry of rice husk derived-biochars. *J. Anal. Appl. Pyrolysis* **2018**, *134*, 281−292.
(10) Natarajan, E. Pyrolysis of Rice Husk in a Fixed Bed Reactor. *World Academy of Science, Engineering and Technology, International Journal of Mechanical and Mechatronics Engineering* **2009**, *3* (2), 2−4.
(11) Cao, X.; Sun, S.; Sun, R. Application of biochar-based catalysts in biomass upgrading: a review. *RSC Adv.* **2017**, *7*, 48793−48805.
(12) Gui, M. S. Z.; Jourabchi, S. A.; Ng, H. K.; Gan, S. Comparison of the yield and properties of bio-oil produced by slow and fast pyrolysis of rice husks and coconut shells. In *Applied Mechanics and Materials*; Trans Tech Publ: 2014 Vol. *625*, pp. 626−629.
(13) Islam, M. N.; Ali, M. H. M.; Haziq, M Fixed bed pyrolysis of biomass solid waste for bio-oil. In *AIP Conference Proceedings*; AIP Publishing LLC: 2017 Vol. *1875*, p 020015.
(14) Wakatuntu, J.; Olupot, P. W.; Jjagwe, J.; Menya, E.; Okure, M. Optimization of pyrolysis conditions for production of rice husk-based bio-oil as an energy carrier. *Results Eng.* **2023**, *17*, No. 100947.
(15) Fadhil, A. B.; Kareem, B. A. Co-pyrolysis of mixed date pits and olive stones: Identification of bio-oil and the production of activated carbon from bio-char. *Journal of Analytical Applied Pyrolysis* **2021**, *158*, No. 105249.
(16) Waqas, S.; Harun, N. Y.; Bilad, M. R.; Samsuri, T.; Nordin, N. A. H. M.; Shamsuddin, N.; Nandiyanto, A. B. D.; Huda, N.; Roslan, J. Response surface methodology for optimization of rotating biological contactor combined with external membrane filtration for wastewater treatment. *Membranes* **2022**, *12*, 271.
(17) Waqas, S.; Harun, N. Y.; Sambudi, N. S.; Arshad, U.; Nordin, N. A. H. M.; Bilad, M. R.; Saeed, A. A. H.; Malik, A. A. SVM and ANN Modelling Approach for the Optimization of Membrane Permeability of a Membrane Rotating Biological Contactor for Wastewater Treatment. *Membranes* **2022**, *12*, 821.
(18) Al-Layla, N. M.; Saleh, L. A.; Fadhil, A. B. Liquid bio-fuels and carbon adsorbents production via pyrolysis of non-edible feedstock. *J. Anal. Appl. Pyrolysis* **2021**, *156*, No. 105088.
(19) Irfan, M.; Waqas, S.; Arshad, U.; Khan, J. A.; Legutko, S.; Kruszelnicka, I.; Ginter-Kramarczyk, D.; Rahman, S.; Skrzypczak, A. Response surface methodology and artificial neural network modelling of membrane rotating biological contactors for wastewater treatment. *Materials* **2022**, *15*, 1932.
(20) Daabo, A. M.; Saeed, L. I.; Altamer, M. H.; Fadhil, A. B.; Badawy, T. The production of bio-based fuels and carbon catalysts from chicken waste. *Renewable Energy* **2022**, *201*, 21−34.
(21) Zhang, L.; Liu, R.; Yin, R.; Mei, Y. Upgrading of bio-oil from biomass fast pyrolysis in China: A review. *Renewable Sustainable Energy Rev.* **2013**, *24*, 66−72.
(22) (a) Weerachanchai, P.; Tangsathitkulchai, C.; Tangsathitkulchai, M. Effect of reaction conditions on the catalytic esterification of bio-oil. *Korean J. Chem. Eng.* **2012**, *29*, 182−189. (b) Xu, W. Y.; Wu, D. Comprehensive utilization of the pyrolysis products from sewage sludge. *Environ. Technol.* **2015**, *36*, 1731−1744.
(23) Greenberg, A. E.; Clesceri, L.; Eaton, A. *Standard methods for the examination of water and wastewater*; American Public Health Association. Inc: 1992.
(24) (a) Bridgwater, A. V. *Advances in thermochemical biomass conversion*; Springer Science & Business Media, 2013 (b) Chen, G.; Leung, D. Y. C. Experimental investigation of biomass waste,(rice straw, cotton stalk, and pine sawdust), pyrolysis characteristics. *Energy Sources* **2003**, *25*, 331−337.
(25) Cheng, S.; Wei, L.; Zhao, X.; Julson, J. Application, deactivation, and regeneration of heterogeneous catalysts in bio-oil upgrading. *Catalysts* **2016**, *6*, 195.
(26) Shaaban, A.; Se, S. M.; Dimin, M. F.; Juoi, J. M.; Husin, M. H. M.; Mitan, N. M. M. Influence of heating temperature and holding time on biochars derived from rubber wood sawdust via slow pyrolysis. *J. Anal. Appl. Pyrolysis* **2014**, *107*, 31−39.
(27) Gupta, S.; Gupta, G. K.; Mondal, M. K. Slow pyrolysis of chemically treated walnut shell for valuable products: Effect of process parameters and in-depth product analysis. *Energy* **2019**, *181*, 665−676.
(28) Sarangi, M.; Nayak, P.; Tiwari, T. N. Effect of temperature on nano-crystalline silica and carbon composites obtained from rice-husk ash. *Composites Part B* **2011**, *42*, 1994−1998.
(29) Isa, K. M.; Daud, S.; Hamidin, N.; Ismail, K.; Saad, S. A.; Kasim, F. H. Thermogravimetric analysis and the optimisation of bio-oil yield from fixed-bed pyrolysis of rice husk using response surface methodology (RSM). *Ind. Crops Prod.* **2011**, *33*, 481−487.
(30) Park, H. J.; Heo, H. S.; Park, Y.-K.; Yim, J.-H.; Jeon, J.-K.; Park, J.; Ryu, C.; Kim, S.-S. Clean bio-oil production from fast pyrolysis of sewage sludge: effects of reaction conditions and metal oxide catalysts. *Bioresour. Technol.* **2010**, *101*, S83−S85.
(31) Heo, H. S.; Park, H. J.; Park, Y.-K.; Ryu, C.; Suh, D. J.; Suh, Y.-W.; Yim, J.-H.; Kim, S.-S. Bio-oil production from fast pyrolysis of waste furniture sawdust in a fluidized bed. *Bioresour. Technol.* **2010**, *101*, S91−S96.
(32) Bunting, B.; Boyd, A. *Pyrolysis oil properties and chemistry related to process and upgrade conditions for pipeline shipment*; Oak Ridge National Laboratory 2012.
(33) (a) Nolte, M. W.; Liberatore, M. W. Viscosity of biomass pyrolysis oils from various feedstocks. *Energy Fuels* **2010**, *24*, 6601−6608. (b) Lira, C. S.; Berruti, F. M.; Palmisano, P.; Berruti, F.; Briens, C.; Pécora, A. A. B. Fast pyrolysis of Amazon tucumã (Astrocaryum aculeatum) seeds in a bubbling fluidized bed reactor. *J. Anal. Appl. Pyrolysis* **2013**, *99*, 23−31.
(34) Samolada, M. C.; Papafotica, A.; Vasalos, I. A. Catalyst evaluation for catalytic biomass pyrolysis. *Energy Fuels* **2000**, *14*, 1161−1167.
(35) Ji-Lu, Z. Bio-oil from fast pyrolysis of rice husk: Yields and related properties and improvement of the pyrolysis system. *J. Anal. Appl. Pyrolysis* **2007**, *80*, 30−35.
(36) Lu, Q.; Yang, X.-L.; Zhu, X.-F. Analysis on chemical and physical properties of bio-oil pyrolyzed from rice husk. *J. Anal. Appl. Pyrolysis* **2008**, *82*, 191−198.

https://doi.org/10.1021/acsomega.3c00868
ACS Omega 2023, 8, 17869−17879

(37) (a) Prajitno, H.; Insyani, R.; Park, J.; Ryu, C.; Kim, J. Non-catalytic upgrading of fast pyrolysis bio-oil in supercritical ethanol and combustion behavior of the upgraded oil. *Appl. Energy* **2016**, *172*, 12−22. (b) Wang, Y.; Akbarzadeh, A.; Chong, L.; Du, J.; Tahir, N.; Awasthi, M. K. Catalytic pyrolysis of lignocellulosic biomass for bio-oil production: A review. *Hemosphere* **2022**, No. 134181.
(38) Zhong, D.; Zeng, K.; Li, J.; Qiu, Y.; Flamant, G.; Nzihou, A.; Vladimirovich, V. S.; Yang, H.; Chen, H. Characteristics and evolution of heavy components in bio-oil from the pyrolysis of cellulose, hemicellulose and lignin. *Renewable Sustainable Energy Rev.* **2022**, *157*, No. 111989.
(39) Geng, Y.; Zhao, Y.; Yue, F.; Zhu, Q.; Xiang, M. A novel method to synthesize pure-phase Si2N2O powders in a fluidized bed reactor. *Ceram. Int.* **2022**, *48*, 33066−33071.
(40) Su, Y.; Liu, L.; Zhang, S.; Xu, D.; Du, H.; Cheng, Y.; Wang, Z.; Xiong, Y. A green route for pyrolysis poly-generation of typical high ash biomass, rice husk: Effects on simultaneous production of carbonic oxide-rich syngas, phenol-abundant bio-oil, high-adsorption porous carbon and amorphous silicon dioxide. *Bioresour. Technol.* **2020**, *295*, No. 122243.
(41) Bakari, R.; Kivevele, T.; Huang, X.; Jande, Y. A. C. Simulation and optimisation of the pyrolysis of rice husk: Preliminary assessment for gasification applications. *J. Anal. Appl. Pyrolysis* **2020**, *150*, No. 104891.
(42) Da Costa, A. A. F.; de Oliveira Pires, L. H.; Padron, D. R.; Balu, A. M.; da Rocha Filho, G. N.; Luque, R.; do Nascimento, L. A. S. Recent advances on catalytic deoxygenation of residues for bio-oil production: An overview. *Mol. Catal.* **2022**, *518*, No. 112052.
(43) Li, H.; Wang, Y.; Zhou, N.; Dai, L.; Deng, W.; Liu, C.; Cheng, Y.; Liu, Y.; Cobb, K.; Chen, P.; Ruan, R. Applications of calcium oxide−based catalysts in biomass pyrolysis/gasification−a review. *J. Cleaner Prod.* **2021**, *291*, No. 125826.
(44) Costa, J. E. B.; Barbosa, A. S.; Melo, M. A. F.; Melo, D. M. A.; Medeiros, R. L. B. A.; Braga, R. M. Renewable aromatics through catalytic pyrolysis of coconut fiber (Cocos nucífera Linn.) using low cost HZSM-5. *Renewable Energy* **2022**, *191*, 439−446.
(45) Staš, M.; Kubička, D.; Chudoba, J.; Pospíšil, M. Overview of analytical methods used for chemical characterization of pyrolysis bio-oil. *Energy Fuels* **2014**, *28*, 385−402.
(46) Lu, R.; Sheng, G.-P.; Hu, Y.-Y.; Zheng, P.; Jiang, H.; Tang, Y.; Yu, H.-Q. Fractional characterization of a bio-oil derived from rice husk. *Biomass Bioenergy* **2011**, *35*, 671−678.
(47) Ren, X.; Meng, J.; Moore, A. M.; Chang, J.; Gou, J.; Park, S. Thermogravimetric investigation on the degradation properties and combustion performance of bio-oils. *Bioresour. Technol.* **2014**, *152*, 267−274.

https://doi.org/10.1021/acsomega.3c00868
ACS Omega 2023, 8, 17869−17879